

# Spontaneous Emission in ultra-cold spin-polarised anisotropic Fermi Seas

Brian O’Sullivan\* and Thomas Busch

*Department of Physics, National University of Ireland, UCC, Cork, Republic of Ireland*

(Dated: October 29, 2018)

We examine and explain the spatial emission patterns of ultracold excited fermions in anisotropic trapping potentials in the presence of a spin polarised Fermi sea of ground state atoms. Due to the Pauli principle, the Fermi sea modifies the available phase space for the recoiling atom and thereby modifies its decay rate and the probability of the emitted photon’s direction. We show that the spatial anisotropies are due to an intricate interplay between Fermi energies and degeneracy values of specific energy levels and identify a regime in which the emission will become completely directional. Our results are relevant for recent advances in trapping and manipulating cold fermionic samples experimentally and give an example of a conceptually new idea for a directional photon source.

PACS numbers: 05.30.-d,67.85.Lm

## I. INTRODUCTION

Cold samples of neutral fermionic atoms have become an important test-bed for a large number of interesting phenomena in many particle physics [1]. Since the first realisation of quantum degeneracy using two spin components of  $^40K$  [2], the field has moved quickly from fundamental quantum statistical experiments [3] into other areas such as BEC-BCS transitions [4], solid state physics [5] and even quark-gluon physics [6].

A particularly impressive achievement has been the realisation that by using a Feshbach resonance it is possible to incite single atoms to pair [7, 8]. Depending on which side of the resonance the experiments are carried out, these pairs then either represent bosonic molecules, which in turn form a Bose-Einstein condensate, or Cooper-pairs, which lead to the formation of a BCS state. By sweeping across a Feshbach resonance one can therefore explore the BEC-BCS crossover regime, which was until recently not experimentally available [4].

Besides molecular or Cooper pair physics, mono-atomic gases have also shown a large potential for demonstrating new and exciting physics. While the most dramatic consequence of the antisymmetry condition on the wave-function of identical fermions is the formation of the Fermi sea at low temperatures, other effects have been predicted and been observed. Among them are the modification of the scattering properties of two atoms, which leads to a reduced efficiency of evaporative cooling [9, 10], narrowing of the line-width of light propagating through the gas [11, 12] and the suppression of off-resonant light scattering [13, 14].

The inhibition of spontaneous emission in the presence of a ground state Fermi sea is another fundamental prediction which results directly from the Pauli principle [14, 15, 16]. In it a degenerate Fermi sea of a spin polarised gas forms the environment for a single, excited

atom of the same kind. Due to the Pauli principle, the Fermi sea effectively blocks out a large amount of the phase space that would otherwise be available to the excited atom after a de-excitation transition. This leads to a modification of the emission properties of the excited atom and the details of the effect are determined by the size of the Fermi sea, the systems temperature and the anisotropy of the trap [16]. The influence on the lifetime of the excited atom has been recently exhaustively investigated [16] and the effect was shown to be an atom-optical analogue of well known effects in cavity QED [17].

In this work we will investigate the influence of this Pauli-blocking effect on the spatial distribution of the emission spectrum of a single atom in an anisotropic trap. The fact that the emission spectrum becomes anisotropic was first shown in [16] and a simple explanation for this effect was given. Here we investigate the pattern formation in detail and in particular consider highly anisotropic traps, which can be achieved today by experimentally using, for example, atom chips or optical lattices [18].

In Sec. II we will first describe the model we are using and, in Sec. III, derive a relation between the Fermi energy and the number of particles in an anisotropic trap. In Sec. IV we describe the effect of the anisotropy on the behaviour of the individual transition elements for spontaneous emission and apply the results to explain the specifics of the overall emission pattern. Finally we conclude.

## II. MODEL

We consider an ideal gas of spin polarised fermions trapped in a harmonic potential. All atoms are assumed to be in their internal ground state,  $|g\rangle$ , so that the gas becomes quantum degenerate at low enough temperatures and forms a perfect Fermi sea at absolute zero. In the following we will restrict our calculations to this limit, as in it the effects we describe are most pronounced and the extension to finite temperatures is, while com-

---

\*Electronic address: bosullivan@phys.ucc.ie

putationally challenging, conceptually straightforward.

In addition to the Fermi sea we assume the presence of a single extra fermion, which is distinguished from the others by being in an internally excited state,  $|e\rangle$ . After some time this atom will spontaneously emit a photon, make a transition into the ground state and become part of the Fermi sea. As all atoms are assumed to be spin polarised, the Pauli principle demands that the new ground state atom has to join the Fermi sea with an energy larger than the Fermi energy. This is an energetically very unfavourable process and the presence of the Fermi sea will therefore lead to an inhibition of the spontaneous emission rate with respect to the case of a free space particle [15, 16].

In the following we will denote the spontaneous emission rate of photons along the direction  $\Omega$  and into the solid angle  $d\Omega$  in the presence of  $N$  ground-state fermions by  $\Gamma(\Omega) d\Omega$  and compare it to the free case ( $N = 0$ ) which we denote by  $\Gamma_0(\Omega) d\Omega$ . Using Fermi's golden rule we can express the excited atom's decay rate as

$$\frac{\Gamma(\Omega)}{\Gamma_0(\Omega)} = \sum_{\vec{n}, \vec{m}=0}^{\infty} P_m (1 - F_n) |\langle \vec{n} | e^{-i\vec{k}(\Omega) \cdot \hat{r}} | \vec{m} \rangle|^2, \quad (1)$$

where  $F_n = (e^{(\hbar\omega/k_B T)(\vec{\lambda} \cdot \vec{n})} + 1)^{-1}$  is the Fermi-Dirac distribution function and  $(1 - F_n)$  is the probability that an energy level  $|n\rangle$  of the harmonic trap is unoccupied.  $P_m = P_0 e^{-(\hbar\omega/k_B T)\vec{\lambda} \cdot \vec{m}}$  is the Boltzmann distribution function describing the single excited fermion in state  $|m\rangle$  of the harmonic trap, which in turn is assumed to have the frequencies  $(\omega_x, \omega_y, \omega_z) \equiv \omega \vec{\lambda}$ . If we restrict eq. (1) to zero temperature the Fermi-Dirac distribution function becomes a step function and hence only states with an energy greater than the Fermi energy have a finite value for  $1 - F_n$ . Similarly, the excited fermion will occupy the ground state of the harmonic trap,  $|m\rangle = |0\rangle$ , and eq. (1) simplifies to

$$M_f(\Omega) = \frac{\Gamma(\Omega)}{\Gamma_0(\Omega)} = \sum_{n=n_F+1}^{\infty} |\langle \vec{n} | e^{-i\vec{k}(\Omega) \cdot \hat{r}} | 0 \rangle|^2, \quad (2)$$

where  $n_F$  represents the Fermi shell. The inhibition of spontaneous emission that results from equation (1) has recently been investigated [16] and here we extend this work by presenting a thorough and detailed investigation into the spatial emission patterns that result from it. This is of interest due to the new parameter ranges which have become experimentally available in recent years. These include, in particular, highly anisotropic traps. While the appearance of a fine structure in the emission patterns was already mentioned in [16], here we derive the framework for its explanation.

We assume that the harmonic oscillator potential has the following standard form

$$V = \frac{M\omega^2}{2} (\vec{\lambda} \cdot \vec{r})^2 = \frac{M\omega^2}{2} (\lambda_x^2 x^2 + \lambda_y^2 y^2 + \lambda_z^2 z^2), \quad (3)$$

where  $M$  is the mass of the particle and the values of  $\lambda_{x,y,z}$  determine the degree of anisotropy in the different directions. For numerical simplicity we will only deal with values of  $\lambda \geq 1$  and restrict ourselves to two types of anisotropic trapping potentials in which two of the axes have identical strength,

$$\lambda_x = \lambda_y = 1 \text{ and } \lambda_z = \lambda, \quad \text{pancake shape,} \quad (4a)$$

$$\lambda_x = \lambda_y = \lambda \text{ and } \lambda_z = 1, \quad \text{cigar shape.} \quad (4b)$$

Due to the symmetries of the pancake and cigar shaped traps about the tight and the soft axes, respectively, eq. (2) can be simplified and expressed in terms of incomplete gamma functions for both trap shapes

$$M_f(\theta) = \frac{\gamma(n_F + 1, \beta)}{\Gamma(n_F + 1)} + e^{-\beta} \sum_{n=0}^{n_F} \frac{\beta^n}{n!} \frac{\gamma(\lfloor \frac{n_F - n}{\lambda} \rfloor + 1, \frac{\alpha}{\lambda})}{\Gamma(\lfloor \frac{n_F - n}{\lambda} \rfloor + 1)}. \quad (5)$$

Here  $\lfloor x \rfloor$  denotes the largest integer less than or equal to  $x$  and  $n_F$  is the quantum number of the Fermi shell, which we will describe in more detail later. For brevity we have defined

$$\alpha = \eta^2 \cos^2 \theta, \quad \beta = \eta^2 \sin^2 \theta \quad \text{pancake shape,} \quad (6a)$$

$$\alpha = \eta^2 \sin^2 \theta, \quad \beta = \eta^2 \cos^2 \theta \quad \text{cigar shape,} \quad (6b)$$

in which  $\eta$  represents the Lamb-Dicke parameter. One can immediately see that the angular distributions for the pancake and the cigar shaped trap can be obtained from each other by a simple  $\pi/2$  rotation, as one would expect. We will make use of this fact when discussing emission patterns in Sec. IV.

### III. DEGENERACIES

Let us first discuss the relationships between the different parameters characterising a Fermi-sea in an anisotropic trap. Since the degeneracies of states with equal energy are a function of the trapping frequencies in the different directions, the relationship between the Fermi energy and particle number is not as straightforward as in the well-known isotropic case.

The eigenenergies of the harmonic potential in eq. (3) are given by

$$E_{n_p} = \left( n_p + \left( \frac{\lambda}{2} + 1 \right) \right) \hbar\omega, \quad (7a)$$

$$E_{n_c} = \left( n_c + \left( \lambda + \frac{1}{2} \right) \right) \hbar\omega, \quad (7b)$$

where we have defined the shell quantum numbers of the pancake and cigar shaped harmonic traps as  $n_p = n_x + n_y + \lambda n_z$  and  $n_c = \lambda n_x + \lambda n_y + n_z$ , respectively. As usual,  $n_x, n_y$  and  $n_z$  refer to the integer quantum numbers of the harmonic oscillator.

As the aspect ratio of a trapping potential is increased the resulting energy levels typically have a reduced degeneracy relative to the isotropic case,  $\lambda = 1$  [19]. For the

purposes of this work, and without loss of generality, we will consider only integer values of  $\lambda$ , allowing us in turn to restrict ourselves to integer values for  $n_{p,c}$ . Therefore we can write the degeneracy for states with fixed energy as

$$g_{n_p} = \frac{1}{2}(\tilde{n}_p + 1)(2n_p - \lambda\tilde{n}_p + 2), \quad (8a)$$

$$g_{n_c} = \frac{1}{2}(\tilde{n}_c + 1)(\tilde{n}_c + 2), \quad (8b)$$

where here and in the following all quantities carrying a tilde take the value of the quantity without the tilde divided by  $\lambda$  and rounded down to the nearest integer, i.e.  $\tilde{x} = \lfloor x/\lambda \rfloor$ . Consequently, the total number of quantum states with an energy equal to and smaller than  $E_{n_F}$  is then given by the sum,

$$S = \sum_{n=0}^{n_F} g_n, \quad (9)$$

which can be calculated to be given by

$$S_p = \frac{1}{6}(\tilde{n}_F + 1)(2n_F - \lambda\tilde{n}_F + 2) \left( \frac{3}{2}n_F - \frac{3}{4}\lambda\tilde{n}_F + \frac{\lambda^2\tilde{n}_F(2 + \tilde{n}_F)}{8 + 8n_F - 4\lambda\tilde{n}_F} + 3 \right), \quad (10a)$$

$$S_c = \frac{1}{6}(\tilde{n}_F + 1)(\tilde{n}_F + 2)(3n_F - 2\tilde{n}_F\lambda + 3). \quad (10b)$$

In our model we assume a spin polarised gas in which each oscillator state is filled with one fermion only. Eqs. (9) therefore determine the number of particles confined for a given Fermi energy  $E_F = n_F\hbar\omega + E_G$ , where  $E_G$  is the ground state energy of the potential.

## IV. EMISSION PATTERNS IN ANISOTROPIC TRAPS

### A. Emission Probabilities.

To understand the emission patterns later on, let us first have a brief look at the emission probabilities of an excited atom in an anisotropic trap. In the presence of an anisotropic Fermi sea the rate of spontaneous emission along a specific direction is determined by three parameters: (1) the number of ground state atoms, (2) the degeneracy of the available states and (3) the Lamb-Dicke parameter  $\eta = \sqrt{E_R/\hbar\omega}$ . The latter determines the range of accessible states and is given by the ratio between the recoil energy,  $E_R = \hbar^2k_0^2/2M$ , and the trapping strength,  $\hbar\omega_{x,y,z}$ , in the different directions. Here  $k_0$  is the wave vector corresponding to the transition  $|e\rangle \rightarrow |g\rangle$ .

In this section we will focus on the influence of the degeneracies of the available states and therefore on the anisotropy of the trap. Let us do this by examining the matrix elements for individual transitions from the

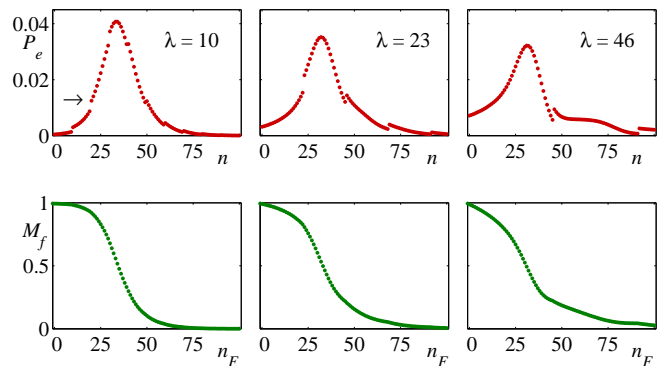


FIG. 1: Top row: emission probability,  $P_e$ , into individual shells in a pancake shaped trap for  $\eta^2 = 36$  and  $\lambda = 10, 23, 46$ . The arrow indicates the  $n = 20$  energy level of the harmonic trap, which is referred to in the text. Bottom row: decay rate of the excited particle,  $M_f$ , for the same parameters as above.

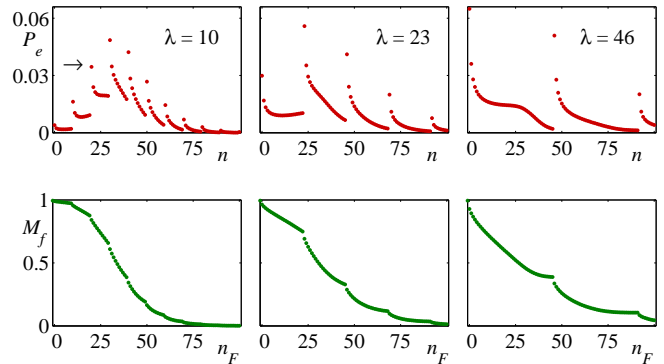


FIG. 2: Top row: emission probability,  $P_e$ , into individual shells in a cigar shaped trap for  $\eta^2 = 36$  and  $\lambda = 10, 23, 46$ . The arrow indicates the  $n = 20$  energy level of the harmonic trap, which is referred to in the text. Bottom row: decay rate of the excited particle,  $M_f$ , for the same parameters as above.

ground cm-state of the excited atom to a single final state,  $|n\rangle$ ,

$$P_e(n) = |\langle n|e^{ikx}|0\rangle|^2. \quad (11)$$

It is well known that for an isotropic trap this distribution is Gaussian in shape and centered around an energy level  $n = \eta^2$ . The effects introduced by an anisotropy are significant and can be clearly seen in the graphs in the upper rows of Figs. 1 and 2, where we show  $P_e$  for a pancake and a cigar shaped trap, respectively, for increasing values of the anisotropy,  $\lambda = 10, 23$  and  $46$ . The most obvious feature in both situations is the appearance of a  $\lambda$ -dependent discontinuity in the distribution, which is more pronounced in the cigar shaped setting.

To explain this behaviour, let us first intuitively argue its existence. When an internally excited atom which is trapped in the ground state of an empty isotropic harmonic trap decays, the probability of the photon being emitted is the same in all directions. This is rather easy

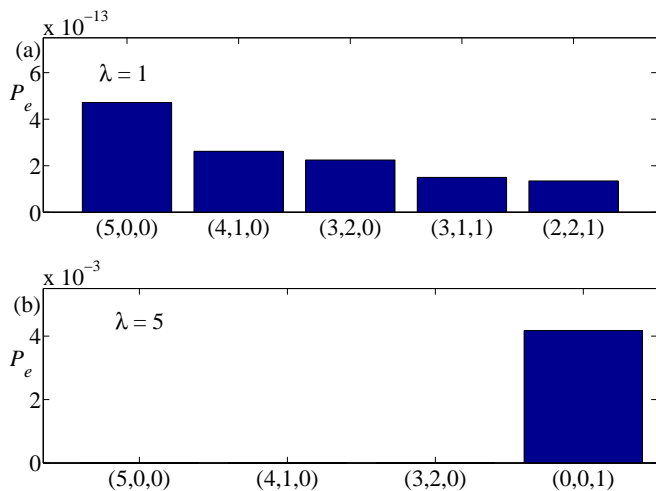


FIG. 3: (a) Emission probability into individual states within the shell  $n = 5$  in an isotropic trap. The triplets represent  $(n_x, n_y, n_z)$  and all permutations of each triplet have the same probability. The Lamb-Dicke factor is  $\eta = 5$ , however changing this value only scales all values. (b) Emission probability into individual states within the shell  $n = 5$  in a pancake trap with  $\lambda = 5$ . The values for the three states on the left are not visible on this scale.

to understand as in this situation the density of states is identical in all directions. However, for the anisotropic trap the situation is different. As the aspect ratio is increased, the degeneracy of any energy level will either decrease or remain the same. Therefore, up to a specific shell the number of quantum states, given by eqs. (9), will be reduced and, as a result, the density of states in the different directions changes. Since the recoil of the de-excited fermion to a certain quantum state and the direction of the emitted photon are directly related, it seems rather surprising that for the free case this emission remains isotropic irrespective of the diminishing number of quantum states. However, it is exactly the modified distribution shown in the upper rows in Figs. 1 and 2 that makes this phenomenon possible.

To gain more insight into the source of the discontinuities let us consider the emission probability into specific states within a degenerate shell  $n$  of an isotropic and a pancake shaped ( $\lambda = 5$ ) trap. Fig. 3 shows  $P_e(n_x, n_y, n_z)$  for a fixed shell, in which all combinations of the triplet (in both (a) and (b)) of quantum numbers adds up to  $n = 5$ . It can be seen that in general states which include ground state excitations have a higher probability for occupation than the ones which do not, which is due to the fact that the excited atom is initially in its centre-of-mass ground state.

When we move from the isotropic to the anisotropic setting it is therefore clear that whenever the value of an energy shell,  $n$ , reaches an integer multiple of the anisotropy parameter, the shell contains a state with two ground state excitations. As these states have a higher

probability of occupation (see Fig. 3(b)) the overall emission probability into this energy shell is increased, leading to the observed discontinuous jump. As an example let us consider a pancake shaped trap with an aspect ratio of  $\lambda = 10$ . For the shell  $n = 19$  (indicated by the arrow in Figs. 1) the degenerate states are  $(n_x + n_y, n_z) = (19, 0)$  and  $(9, 1)$ , whereas for the  $n = 20$  energy level states are  $(n_x + n_y, n_z) = (20, 0)$ ,  $(10, 1)$  and  $(0, 2)$ . The extra  $(0, 2)$  state is the dominant contributor and its appearance responsible for the discontinuous increase in the emission probability. For the cigar trap this effect is even more pronounced as there are two tight directions and in the example above the states  $(n_x, n_y, n_z) = (2, 0, 0)$  and  $(0, 2, 0)$  become both available.

For completeness we show the integrated emission probability for increasing particle number (i.e. increasing Fermi energy or Fermi level) and different anisotropies in bottom rows of Figs. 1 and 2. Fermi inhibition is absent for the empty trap ( $M_f = 1$ ), shown for  $n_F = -1$ , slowly increases for  $n_F \geq 0$  and accelerates for  $n_F \sim \eta^2$ . The discontinuity in the variable  $P_e(n)$  translates clearly into non-smooth kinks in this distribution.

## B. Emission along Tight and Soft Axes.

The fact that the presence of an anisotropic Fermi sea will lead to anisotropic emission patterns was already noted in [16] and in the following we will develop a detailed understanding of the directional features. Since for the pancake as well as for the cigar shaped trap the emission is isotropic around their respective symmetry axis,  $(0, \pi)$ , we can treat both geometries in a quasi 2D picture. It is then immediately clear that the results for both settings will be related by a simple  $\pi/2$  rotation (due to our definition of  $\lambda \geq 1$ ).

Let us first look at the emission along the principal axes of the anisotropic trap in the tight and the soft direction. Choosing the tight direction in the pancake (cigar) shaped trap along  $\theta = 0$  ( $\theta = \pi/2$ ) the modification factor in eq. (5) simplifies to

$$M_f = \frac{\gamma(\tilde{n}_F + 1, \frac{\eta^2}{\lambda})}{\Gamma(\tilde{n}_F + 1)}. \quad (12)$$

The behaviour of this equation with increasing anisotropy is shown in Fig. 4 for a system with  $n_F = 60$ . The most obvious feature of the plot is a series of sawtooth-like discontinuities. Careful examination shows that  $n_F$  of these exist and they appear whenever the value of the aspect ratio,  $\lambda$ , increases beyond the values of  $\frac{n_F}{m}$ , ( $m = 1, 2, \dots, n_F$ ). The increase in emission probability for values just after this point is due to the availability of an extra free state with a lower tight excitation just outside the Fermi edge. For example, in the pancake trap, when one moves from  $\lambda = 30$  to  $\lambda > 30$  the state  $(n_x + n_y, n_z) = (0, 2)$  emerges from the Fermi sea for  $n_F = 60$ . As discussed in Section IV A, this state has a



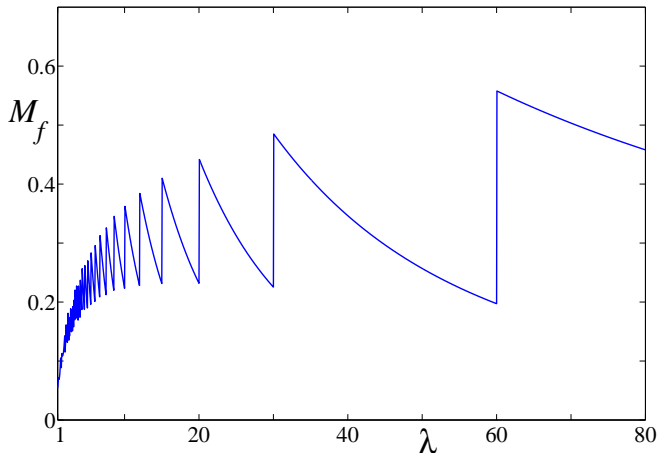


FIG. 4:  $M_f$  along the tight axis at  $T = 0$ .  $\eta^2 = 49$ ,  $n_F = 60$ . Note that we use a continuous distribution of  $\lambda$  for this graph.

high probability to be emitted into as it contains ground state excitations in the soft direction, hence the large increase in the decay rate. By increasing  $\lambda$  further this state moves away from the Fermi edge, and the emission probability decreases until the next state with a lower tight excitation, emerges from the Fermi sea. For values of  $\lambda > n_F$  no more discontinuities appear since the Fermi sea only occupies energy states with ground state excitations in the tight direction. Emission along the soft direction can be calculated from eq. (12) by taking  $\lambda = 1$  and the decay rate along this direction is determined exclusively by the Fermi shell  $n_F$  and the value of the Lamb-Dicke parameter  $\eta$ .

Considering a fixed value of the aspect ratio  $\lambda$  in either anisotropic trapping potential and changing  $n_F$  one notices a degeneracy in the emission probability in the tight direction, shown in Fig. 5(a). This behaviour was already mentioned in [16] and we can see from eq. (12) that it stems from the fact that  $\tilde{n}_F$  only changes its value in steps of  $\lambda$ . An increase in the value of  $\tilde{n}_F$  coincides with the Fermi sea occupying a state with a higher tight excitation (and ground state soft excitations), leading to a decrease in the decay rate along the tight direction. For example, when moving from  $n_F = 35$  to  $n_F = 36$  the state  $(n_x + n_y, n_z) = (0, 9)$  becomes occupied by the Fermi sea, producing the discontinuous reduction of the decay rate (see Fig. 5(a)).

### C. Fine Structure

The emission spectrum between the principal axes is characterised by the appearance of a fine structure (see Fig. 5(b)), which exists for a wide range of parameters. The first hint to understanding the origins of the visible extrema comes from noticing that the number of maxima between the soft and tight axes is related to the number of excitations in the tight direction that are occupied by

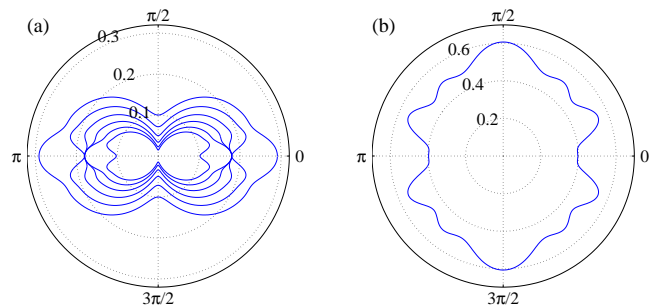


FIG. 5: (a)  $M_f(\theta)$  in a pancake shaped trap at  $T = 0$ .  $\eta^2 = 25$ ,  $\lambda = 4$  with  $n_F = 31$  (outermost) to  $n_F = 36$  (innermost). (b)  $M_f(\theta)$  in a pancake shaped trap with  $\lambda = 11$ ,  $\eta^2 = 25$  and  $n_F = 23$ .

the Fermi sea,  $\tilde{n}_F$ . To show this relation let us consider the emission probability into shells with a fixed value for  $n_z$  in a pancake shaped trap

$$M_f(\theta, n_z) = e^{-\frac{\alpha}{\lambda}} \frac{\left(\frac{\eta^2}{\lambda}\right)^{n_z}}{n_z!} \frac{\gamma(\max(0, n_F - \lambda n_z + 1), \beta)}{\Gamma(\max(0, n_F - \lambda n_z + 1))} \quad (13)$$

with the definition of  $\alpha$  and  $\beta$  given in eqs. (6). As a specific example we show in Fig. 5(b) a gas with  $n_F = 23$ ,  $\eta^2 = 25$  and  $\lambda = 11$ . In this case we find  $\tilde{n}_F = 2$  maxima in the  $\pi/2$  arc between the tight to the soft axis. Comparing this emission pattern to the results from eq. (13), one can see (Fig. 6) that each isolated contribution from a transition into a state with a fixed value of  $n_z$  is responsible for one of the maxima. For values of  $n_z > \tilde{n}_F$  the emission is predominantly into the tight direction, therefore originating from transitions into states for which both ground state excitations in the soft direction are available. Similarly, when restricting the recoiling atom to occupying states with a ground state excitation in the tight direction,  $n_z = 0$ , the emission is mainly focussed around small angles about the soft axis. The intermediate excitations,  $n_z = 1, 2$ , make up the two intermediate ripples between the principle axes and summing up the contributions to the photon emission of all four plots in Fig. 6 gives the emission plot shown in Fig. 5(b). In contrast, if we calculate eq. (13) for an isotropic trap for different values of  $n_z$ , each individual term would show a similar behaviour of having a single maximum at a finite angle between the principle axes. However, the sum of those will give the isotropic emission pattern which corresponds to the decay rate being the same in all directions.

It is now obvious that for the limit  $\lambda > n_F$  the fine structure disappears and the extrema of emission will be located around the directions of the principal axes (see Fig. 7(a)). As  $\lambda \rightarrow \infty$ , emission into the tight direction is reduced, whereas the emission in the soft direction remains constant, Fig. 7(b). In this regime the Fermi sea is completely confined to states with ground state excitations in the tight direction. Therefore, it becomes easier for the recoiling atom to access states in the soft direction due to the diminishing density of states in the tight

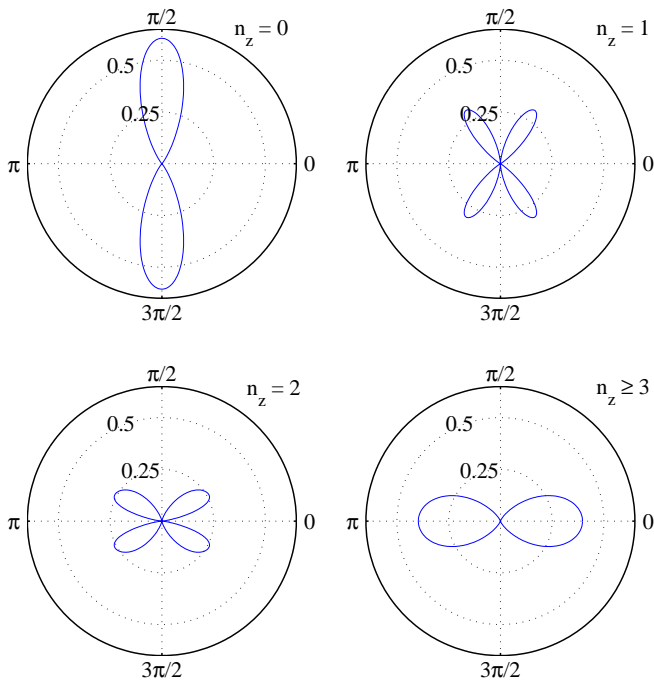


FIG. 6:  $M_f(\theta, n_z)$  for a pancake shaped trap with,  $\lambda = 11$ ,  $\eta^2 = 25$  and  $n_F = 23$ . In the four graphs the decay is only allowed into quantum states of the harmonic trap with  $n_z = 0, 1, 2$ , and  $n_z \geq 3$ , respectively.

direction. In the limit of  $\lambda \rightarrow \infty$  the emission probability can be written as

$$M_f(\theta; \lambda \rightarrow \infty) = \frac{\gamma(n_F + 1, \beta)}{\Gamma(n_F + 1)}, \quad (14)$$

and it shows that the emission probability in the tight direction has completely vanished.

It is possible to make use of this behaviour and create a system where photon emission become highly directional. While directional photon emission is usually achieved by using optical cavities (and therefore engineering the Hilbert space of the photon), this example is complementary in that it uses a cavity (trap) for the atoms and thereby engineers the Hilbert space of the particles. Let us stress that it is not primarily the size of the Fermi sea that is responsible for this effect, merely the presence of the Fermi sea. The emission probability of the photon can still be close to the emission probability in free space whilst  $\eta^2 \gtrsim n_F$ . (see Fig. 7(a)). As the emission is symmetric through a  $2\pi$  rotation about the  $(0, \pi)$  axis in the above example, we display the 3D emission probability in Fig. 7(b). Also note that for a pancake shaped trap this effect would correspond to emission into a well defined plane perpendicular to the tight principal axis.

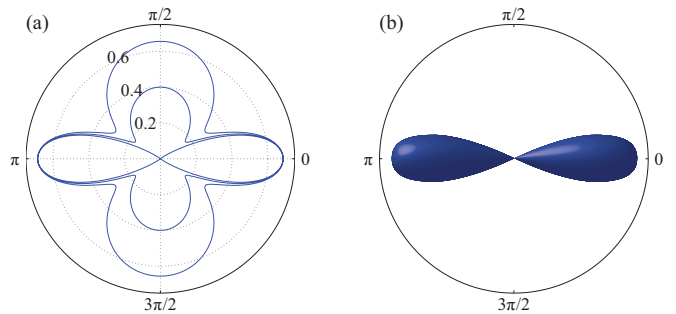


FIG. 7: (a)  $M_f(\theta)$  in a cigar shaped trap at  $T = 0$  with  $n_F = 45$  and  $\eta^2 = 49$ .  $\lambda = 46$  (outermost),  $\lambda = 96$  (center plot) and  $\lambda = \infty$  (innermost). The plot is symmetric through a  $2\pi$  rotation about the  $(0, \pi)$  axis. (b) A three-dimensional illustration of the excited particles decay rate in a cigar trap in the large anisotropy limit.

## V. CONCLUSION

In this work we have given a detailed investigation into the spatial properties of spontaneous emission of a single atom in the presence of an anisotropic, ideal and spin polarised ultracold Fermi gas. The demand to obey the Pauli principle leads to the formation of a non-trivial, anisotropic emission pattern for the photon, which can be explained by carefully examining the allowed transitions the recoiling atom can make.

We have first calculated the relation between the Fermi energy and the particle number and then investigated the single particle transition matrix element, for both geometries of anisotropic traps. The change in the density of states into the different spatial directions was found to be accompanied by the appearance of discontinuities in the distribution of the emission probability spectrum for different shells. While in an isotropic trap these two effects cancel and produce an isotropic emission spectrum, in an anisotropic trap they lead to an intricate fine-structure in the presence of a Fermi sea.

In a next step we have managed to explain this fine-structure by attributing the extrema to the emissions which come from the transitions of the recoiling atom into well defined states in the tight direction. If the aspect ratio exceeds the Fermi energy, the fine-structure vanishes and the emission spectrum becomes smooth, though not isotropic, again.

Finally, we have pointed out that this system can be used to create a highly directional photon source. The effect uncovered is complementary to the common use of optical cavities to influence a photons direction after emission and makes use of the ability to influence the atom's phase space. The experimental observation of directional photon emission in anisotropic, cold, fermionic gases would therefore be a sign of a fundamental consequence of the symmetry of fermionic particles.

## VI. ACKNOWLEDGEMENTS

We would like to thank T. Ramos for valuable discussions. This project was supported by Science Founda-

tion Ireland under project number 05/IN/I852. BOS acknowledges support from IRCSET through the Embark Initiative RS/2006/172.

- 
- [1] S. Giorgini, L.P. Pitaevskii, and S. Stringari, arXiv:0706.3360v2.
  - [2] B. DeMarco and D.S. Jin, *Science* **285**, 1703 (1999).
  - [3] A.G. Truscott, K.E. Strecker, W.I. McAlexander, G.B. Partridge, and R. G. Hulet, *Science* **291**, 2570 (2001).
  - [4] W. Ketterle and M.W. Zwierlein, *Ultracold Fermi Gases, Proceedings of the International School of Physics "Enrico Fermi", Course CLXIV, Varenna, edited by M. Inguscio, W. Ketterle, and C. Salomon (IOS Press, Amsterdam) 2008.*
  - [5] I. Bloch, J. Dalibard, and W. Zwerger, *Rev. Mod. Phys.* **80**, 885 (2008).
  - [6] E.V. Shuryak, *Nucl. Phys. A* **750**, 64 (2005).
  - [7] G.M. Bruun, and C.J. Pethick, *Phys. Rev. Lett.* **92**, 140404 (2004).
  - [8] T. Köhler, K. Goral, and P.S. Julienne, *Rev. Mod. Phys.* **78**, 1311 (2006).
  - [9] G. Ferrari, *Phys. Rev. A* **59**, R4125 (1999).
  - [10] B. DeMarco, S.B. Papp, and D.S. Jin, *Phys. Rev. Lett.* **86** 5409 (2001).
  - [11] J. Ruostekoski and J. Javanainen, *Phys. Rev. Lett.* **82**, 4741 (1999).
  - [12] J. Javanainen, J. Ruostekoski, B. Vestergaard, and M.R. Francis, *Phys. Rev. A* **59**, 649 (1999).
  - [13] B. DeMarco and D.S. Jin, *Phys. Rev. A* **58**, R4267 (1998).
  - [14] A. Görlitz, A.P. Chikkatur, and W. Ketterle, *Phys. Rev. A* **63**, 041601 (2001).
  - [15] K. Helmerson, M. Xiao, and D. Pritchard, *IQEC'90 book of abstracts, QTHH4, (1990).*
  - [16] Th. Busch, J.R. Anglin, J.I. Cirac, and P. Zoller, *Europhys. Lett.* **44**, 1 (1998).
  - [17] E.M. Purcell, *Phys. Rev.* **69**, 681 (1946).
  - [18] S. Aubin, S. Myrskog, M.H.T. Extavour, L.J. LeBlanc, D. McKay, A. Stummer and J.H. Thywissen, *Nature Physics* **2**, 384 (2006).
  - [19] C. Cohen-Tannoudji, B. Diu, and F. Laloë, *Quantum Mechanics, Vol. 1., pp. 550*, New York: Wiley, 1977.